Journal of Advanced Marine Engineering and Technology, Vol. 50, No. 2, pp. 129~137, 2026
J. Advanced Marine Engineering and Technology (JAMET)
https://doi.org/10.5916/jamet.2026.50.2.129

ISSN 2234-7925 (Print)
ISSN 2765-4796 (Online)
Original Paper

Design of pure-radial vertical profile ring rolling process for manufacturing support rings

In-Kyu Lee[1] · Sang-Kon Lee[2] · Sung-Yun Lee[3] · Kyung-Hun Lee[†]

(Received February 10, 2026 ; Revised March 30, 2026 ; Accepted April 26, 2026)

Abstract: In this study, a design method has been developed to manufacture support rings in a pure-radial vertical profile ring rolling process, based on a feasible forming condition and a uniform volume distribution element technique (UVDET). First, a mathematical model for the pure-radial ring rolling process was developed, assuming the volume constancy of the metal and the growth rate of the ring outer diameter. Second, the feasible forming conditions were derived based on mathematical modeling that comprehensively deals with metal plastic penetration and force equilibrium. Finally, the material flow during the profile ring rolling process was controlled through initial ring blank redesign using UVDET. To verify the proposed process, we carried out finite element (FE) simulations by developing reliable three-dimensional FE-analysis models using Forge Nxt 3.2 commercial software. The results of FE-analysis show that the designed process leads to a successful support ring shape, higher dimensional precision, and efficient plastic penetration.

Keywords: Vertical profile ring rolling, Feasible forming condition, Uniform volume distribution element technique, Support ring, Finite element analysis

1. Introduction

A hot ring rolling is a representative progressive metal forming process, and various types of ring mills exist, including vertical, horizontal, and multi-mandrel ring rolling mills. Early horizontal ring rolling mills were primarily pure-radial ring rolling mills, which performed only radial deformation using a main roll and mandrel. Currently, most ring rolling mills are radial-axial ring rolling mills, which utilize a pair of axial rolls to reduce the ring height in addition to circumferential forming using a main roll and mandrel. Recent research has also focused on radial-axial ring rolling mills **[1]-[5]**. However, this research aims to develop a ring rolling process control algorithm applicable to pure-radial ring rolling mills, which are widely used by domestic small and medium-sized enterprises to produce small-scale ring supports, and to design a ring rolling process that minimizes fishtail defects.

In a conventional plain ring rolling process, the outer surface of the rolls is flat, so that the ring's thickness and outer diameter can be adjusted without altering the ring's outer surface shape, while still producing a ring product of the required diameter. A typical ring rolling mill consists of a main roll that transmits torque to the ring blank to rotate it circumferentially, a mandrel that rotates without driving and applies a forming load in the radial direction to the material, and a pair of axial rolls that deform the upper part of the material to control axial plastic deformation. Using this equipment, the initial ring blank is placed between the mandrel and the main rolls. As the main rolls rotate and apply compressive force to the mandrel, the distance between the rolls narrows, thereby thinning the ring. Since the volume of the material remains constant during deformation, the ring's thinning is compensated for by an increase in its diameter. In this study, a pure-radial vertical ring rolling mill was used, omitting a pair of axial rolls, which made it difficult to control axial plastic deformation. Accordingly, it is necessary to establish a roll control standard to ensure the stability of the ring rolling process along with a

† Corresponding Author (ORCID: http://orcid.org/0000-0001-6474-527X): Professor, Division of Coast Guard Studies, Korea Maritime & Ocean University, 727, Taejong-ro, Yeongdo-gu, Busan 49112, Korea, E-mail: submarine@kmou.ac.kr, Tel: +82-51-410-4263
1 Principal researcher, Advanced Mobility & Robot Components Group, Daegu Production Technology Support Center, Korea Institute of Industrial Technology, E-mail: lik1025@kitech.re.kr, Tel: +82-53-580-0173
2 Principal researcher, Advanced Mobility & Robot Components Group, Daegu Production Technology Support Center, Korea Institute of Industrial Technology, E-mail: sklee@kitech.re.kr, Tel: +82-53-580-0136
3 Principal researcher, Advanced Mobility & Robot Components Group, Daegu Production Technology Support Center, Korea Institute of Industrial Technology, E-mail: yunskills@kitech.re.kr, Tel: +82-53-580-0196

pure-radial ring rolling process control algorithm **[6]**.

The profile ring rolling process is an extremely challenging metal plastic forming process that requires simultaneously achieving the required ring cross-sectional shape while the initial ring blank's outer diameter is deformed to reach the required dimensions. Furthermore, the support ring, a product developed in this research and development with a vertically asymmetrical cross-section, has a short diameter that does not allow for a sufficient forming section. Bending defects and over/under-filling defects present significant challenges in process control and ring blank shape design. Typically, ring rolling dies (main roll, mandrel) and ring blank shape design have relied heavily on field experience. Moreover, the process design of a profile ring rolling using finite element (FE) analysis can be inefficient due to the difficulty of constructing sound FE-analysis models and extremely long computational times **[7]-[10]**.

Therefore, this study first proposes a mathematical model of the feasible forming conditions that determines the mathematical correlations among the rolls and the reasonable ranges of the main roll feed rate, based on the mean thickness-to-length ratio of the plastic deformation zone. Second, the influence of principal design variables, such as the main roll rotation speed and roll radius, on the main roll feed rate was evaluated using the Taguchi method. Finally, a theoretical analysis-based design method utilizing the uniform volume distribution element technique (UVDET) was proposed to design the initial ring blank shape for the ring rolling process, considering metal flow. The proposed design method was inspected by profile ring rolling FE-analysis for manufacturing support rings using S45C steel alloys.

2. Design of Pure-radial Vertical Profile Ring Rolling Process

2.1 Development of FE-analysis Model

Using field data gathered from an actual on-site manufacturing facility, a FE-analysis model of the hot vertical ring rolling process for support ring manufacturing was developed, and forming analysis was performed. The hot ring rolling mill is currently in use, and its initial settings are shown in **Figure 1**. This pure-radial ring rolling mill consists of a main roll, a mandrel, and a pair of centering rolls. The ring rolling mill is a mandrel-mounted type, with the upper main roll rotating and moving downward at a constant speed. The hot ring rolling process was analyzed using Forge Nxt 3.2 software, and the FE-analysis results were compared with the experimental results, thereby verifying the validity of the FE-analysis model.

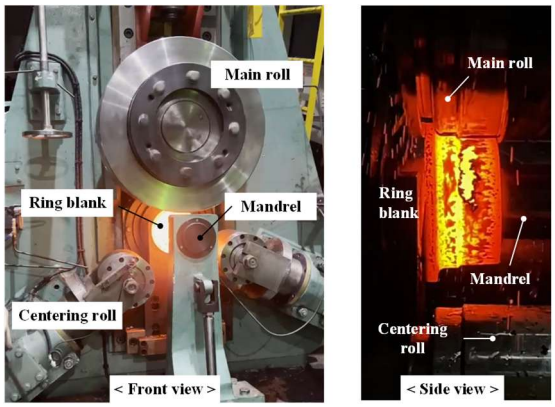

Figure 1: Pure-radial vertical hot ring rolling mill

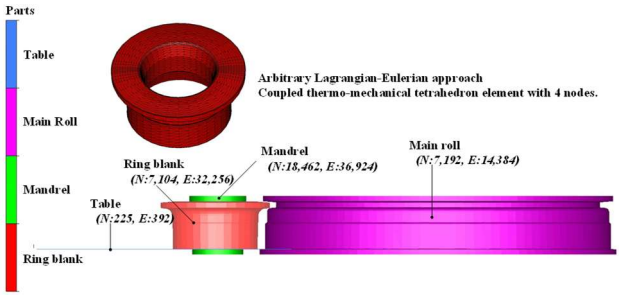

Figure 2: 3D FE-analysis model for profile ring rolling process

2.1.1 FE-analysis Model

A 3D FE-analysis model of a pure-radial vertical profile ring rolling process was constructed, as shown in **Figure 2**, by applying the rolls and process conditions currently used by an actual on-site manufacturing facility for manufacturing support rings. Each roll is set as a rigid body. The main roll rotates at a constant rotational speed of 30 rpm and moves at a maximum speed of 2.25 mm/s in the thickness direction of the ring blank. The mandrel rotates idly around its axis but is stationary. The centering roll option, which restricts the movement of the ring blank during the ring rolling process, is activated. The Coulomb friction model is applied to the friction at the contact surface between the main roll and the ring and is set to the no-lubricant friction condition for the hot forging of Forge Nxt 3.2. Since the mandrel rotates at the same linear speed as the ring blank, it is assumed to have a smooth surface in most ring rolling process analyses.

To resolve convergence issues during the forming analysis and minimize computational time, the arbitrary Lagrangian-Eulerian (ALE) approach and a four-node coupled thermomechanical tetrahedron element were adopted for model calculations. The number of nodes and elements in the ring blank is 7,104 and 32,256,

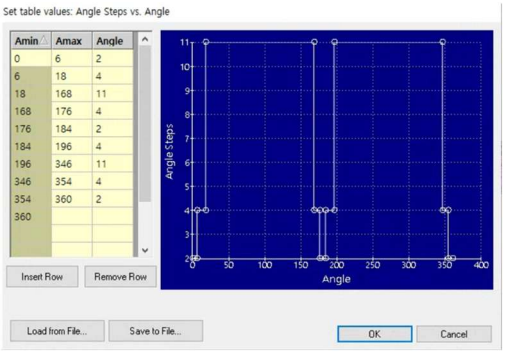

Figure 3: Set table values of ALE approach: angle steps vs angle

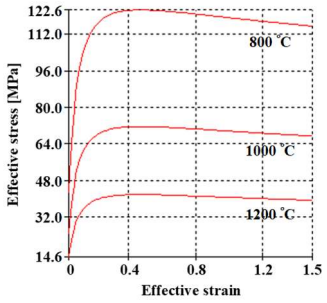

(a) strain rate: $0.1s^{-1}$

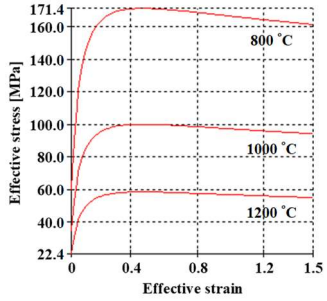

(b) strain rate: $1s^{-1}$

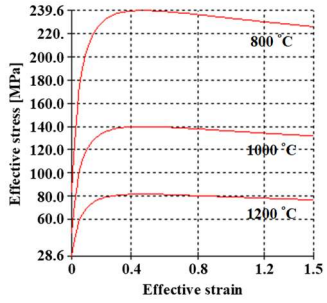

(c) strain rate: $10s^{-1}$

Figure 4: Stress-strain curves of S45C under different temperatures and strain rates

respectively. The angle step in the circumferential direction of the ring blank for the ALE approach is shown in **Figure 3**. The minimum value of 1 was set between the driving roll and the mandrel, which are the main deformation regions.

Table 1: Input parameters for FE-analysis

Parameter	Value
Ring material	S45C
Friction coefficient	0.3
Outermost radius of main roll	339.4 mm
Innermost radius of main roll	317.85 mm
Outermost radius of mandrel	56.03 mm
Innermost radius of mandrel	50 mm
Temperature of ring blank	900°C
Temperature of rolls	250°C
Rotational speed of main roll	30 rpm

The material used in the FE-analysis, S45C, has an elastic modulus and Poisson's ratio of 200GPa and 0.3, respectively, and a density of 7,850kg/m^3. **Figure 4** shows the stress-strain curve according to temperature and strain rate. The hot deformation behavior of S45C steel alloy represents a material property embedded in FORGE Nxt 3.2 and is modeled by the Hensel-Spittel constitutive equation. The temperature-dependent physical properties confirmed by Metal Supplier Online of America are as follows: specific heat of 778 J·kg^{-1}·°C, thermal conductivity of 35.5 W·m^{-1}·C^{-1}, and emissivity of 0.88. The initial ring blank and each roll temperature were set to 900˚C and 250˚C, respectively. The main process variables of ring mills used in industrial settings are shown in **Table 1**.

2.1.2 Results of FE-analysis

The shape changes of the support ring product formed under FE-analysis conditions identical to the field operation conditions are shown in **Figure 5**. The effective strain distribution at each step was set to the auto range, and the minimum and maximum strain values at the last step (15 sec) were observed to be 0.776 and 3.726, respectively. Sound deformation proceeded without any significant defects up to the step (10 sec) of two-thirds of the total travel distance of the main roll. As can be seen in the plastic zone distribution in **Figure 5**, deformation first begins at the outer protrusion (Part A) of the support ring. Thereafter, the contact (deformation) zone gradually increases toward the lower part (Part B) of the support ring. During the ring rolling process, the ring blank thickness is reduced by the compressive force in the thickness direction as it begins to contact the main roll (or mandrel). As the thickness is reduced, the ring blank must exhibit material flow in the axial and circumferential directions. The axial material flow was restricted by the end of the drive roll (Part C) used in this analysis model, while the circumferential flow was accelerated. This difference in diameter growth rates between the upper and lower ring sections resulted in a lifting defect in the support ring after the analysis was completed (15 seconds). The

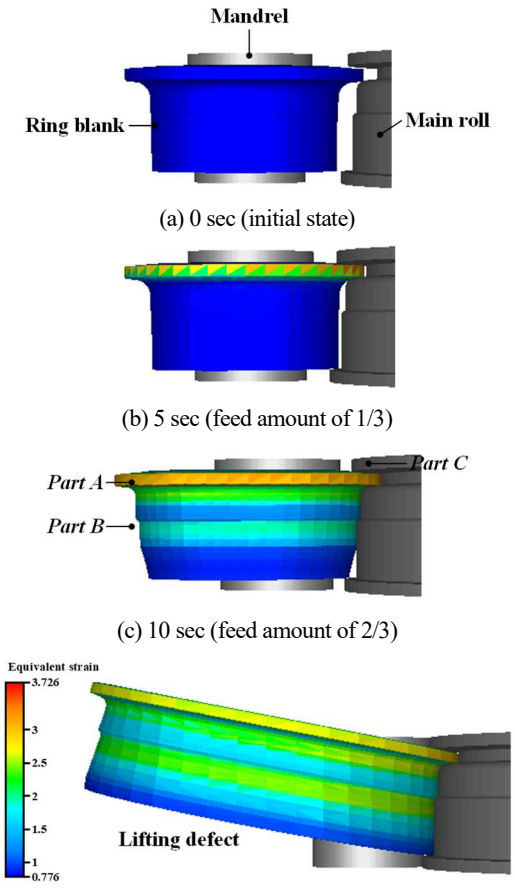

(a) 0 sec (initial state)

(b) 5 sec (feed amount of 1/3)

(c) 10 sec (feed amount of 2/3)

(d) 15 sec (feed amount 3/3)

Figure 5: Plastic zone distribution of deformed support ring during ring rolling process

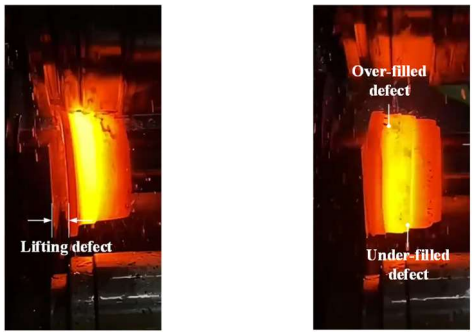

(a) 15 sec (b) after whole process

Figure 6: Deformed ring configuration

diameter growth rate and material flow along the ring height should be considered during redesign.

Figure 6 shows the experimental results of the hot vertical ring rolling process for manufacturing support rings. Lifting defects identical to those observed in the FE-analysis result were observed in the try-out process, and the stability of the ring rolling process was degraded, resulting in uneven support ring thickness and overfilling/underfilling defects.

2.2 Mathematical Model for Pure-radial Vertical Ring Rolling Process

The principal design parameters for developing a control algorithm for a pure-radial vertical ring rolling process are as follows. The ring rolling process is driven by the complex interaction of the dimensions of an initial ring blank, final product, and each roll, the rotational speed of the main roll, the feed speed of the main roll, and the position of centering rolls. The effects of gravity are ignored during process control.

This research proposed a mathematical model based on the roll feed speed and the ring diameter growth rate and used it to design a ring rolling process that minimizes material defects. For the initial ring blank temperature, industrial field data were analyzed and applied to the process design within the allowable temperature range. A typical pure-radial vertical ring rolling process control algorithm is as follows. Additionally, when applied to a profile ring rolling process, the cross sections of the ring blank and the final product can be assumed to be rectangular using the equivalent sphere conversion method, allowing the same control algorithm to be utilized **[5]-[6]**.

(i) Input the initial values for the ring rolling mill, ring blank dimensions, and the rotation speed of the main roll. The outer diameter of the initial ring blank, D_0, thickness(width), S_0, and height, H_0; the outer diameter of the ring-rolled product, D_f, thickness, S_f, and height, H_f; the radius of the main roll, R_{main}; the radius of the mandrel, $R_{mandrel}$; the rotation speed of the main roll, N_{main}; and the increase speed of the ring outer diameter, dD/dt.

(ii) If the mass loss due to oxide scale generated during the ring rolling process is ignored, the volume of the ring is always constant. C_0 and C_i are the initial and instantaneous volumes of the ring blank, respectively.

$$C_0 = (D_0 - S_0) \cdot S_0 \cdot H_0 = C_i \tag{1}$$

(iii) Calculate the instantaneous thickness, S_i, height, H_i, and outer diameter of the ring blank, D_i during the pure-radial vertical ring rolling process. Therefore, for i = 1, 2, …, n, the following equation holds:

$$\begin{aligned} S_i &= S_{i-1} + (S_f - S_0)/n \\ H_i &= H_0 = H_f \\ D_i &= C_i/(\pi \cdot S_i \cdot H_i) + S_i \end{aligned} \tag{2}$$

(iv) Calculate the time, t_i, based on the ring outer diameter growth

rate and the ring dimensions calculated in the previous step.

$$t_i = t_{i-1} + (D_i - D_{i-1})/\left(dD/dt_i\right) \quad (3)$$

(v) The feed rate of the main roll, $V_{main,i}$, is calculated based on the thickness, height of the ring blank, and the time that changes during the ring rolling process.

$$V_{main,i} = \frac{1}{2}\left[\left(\frac{S_{i+1}-S_i}{t_{i+1}-t_i}\right) + \left(\frac{S_i-S_{i-1}}{t_i-t_{i-1}}\right)\right] \quad (4)$$

2.3 Feasible Forming Condition for Pure-radial Vertical Ring Rolling Process

During the pure-radial ring rolling process, changes in the plastic deformation zone of the ring blank and the occurrence of material defects are closely related to the feed amount and feed rate. If the feed amount per rotation of the main roll is too small, the plastic zone will only occur at the contact area with the rolls. The deformation zone cannot sufficiently penetrate, limiting plastic deformation to the center of the ring thickness. Consequently, the ring's outer diameter cannot expand, which can lead to maternal defects. It is necessary to define the minimum required feed amount and the corresponding minimum feed rate of the main roll to ensure a plastic zone across the entire ring thickness **[5]-[6]**.

$$\Delta S_{min} = 1 \times 10^{-2} \cdot (R_i - r_i)^2 \cdot \left(\frac{1}{R_{main}} + \frac{1}{R_{mandrel}} + \frac{1}{R_i} - \frac{1}{r_i}\right) \quad (5)$$

$$\Delta V_{min} = 1 \times 10^{-2} \cdot N_{main} \cdot \frac{R_{main}}{R_i} \cdot (R_i - r_i)^2 \cdot \left(\frac{1}{R_{main}} + \frac{1}{R_{mandrel}} + \frac{1}{R_i} - \frac{1}{r_i}\right) \quad (6)$$

where R_i and r_i are the instantaneous outer and inner radii of the ring blank, respectively.

In the ring rolling process, the ring blank must be continuously fed between the main roll and the mandrel. Therefore, the axial force in the rolling direction must always be relatively higher than the pressing force in the thickness direction. Furthermore, the force in the feed direction of the main roll must be balanced. Based on the above force equilibrium equation, the maximum feed amount and the resulting maximum feed rate of the main roll must be defined.

$$\Delta S_{max} = \frac{2(arctan\mu)^2 \cdot R_{main}}{(1+R_{main}/R_{mandrel})}\left(\frac{1}{R_{main}} + \frac{1}{R_{mandrel}} + \frac{1}{R_i} - \frac{1}{r_i}\right) \quad (7)$$

$$\Delta V_{max} = \frac{2(arctan\mu)^2 \cdot N_{main} \cdot R_{main}^2}{R_i \cdot (1+R_{main}/R_{mandrel})}\left(1 + \frac{R_{main}}{R_{mandrel}} + \frac{R_{main}}{R_i} - \frac{R_{main}}{r_i}\right) \quad (8)$$

Therefore, the feasible forming condition for minimizing the fishtail defects in a pure-radial vertical ring rolling process is calculated as shown in **Equation (9)** below.

$$\Delta V_{min} \le V_{main} \le \Delta V_{max} \quad (9)$$

2.4 Taguchi Design Analysis for Influence of Process Variables

To investigate the influence of the main design variables on the feasible forming conditions, the levels of the design variables were set within the range actually applied in the field, as shown in **Table 2**. **Table 3** shows a four-level orthogonal array table for the three design variables. **Figure 7** shows the factor influence by level as a result of applying the Taguchi method. Among the three design variables (N_{main}, R_{main}, $R_{mandrel}$), the rotation speed of the main roll had the greatest influence, and as the rotation speed increased, the minimum/maximum feed rate increased. The influences of the remaining design variables, the radius of the main roll and the radius of the mandrel, were somewhat low, but the radius of the mandrel and the radius of the main roll showed slightly stronger influences on the minimum feed rate and the maximum feed rate, respectively.

Table 2: Values of design variables at each level

Variables	Level 1	Level 2	Level 3	Level 3
N_{main} [rpm]	10	20	30	40
R_{main} [mm]	250	300	350	400
$R_{mandrel}$ [mm]	40	50	60	70

Table 3: $L_{16}(3^4)$ orthogonal array

No. of case	V_{min} [mm/s]	V_{max} [mm/s]
1	0.532	13.899
2	0.490	19.778
3	0.455	26.251
4	0.425	33.135
5	0.846	32.266
6	1.242	33.991
7	0.766	57.226
8	1.016	61.768
9	1.051	54.050
10	1.022	72.299
11	2.130	60.30
12	1.874	81.292
13	1.194	78.404
14	1.612	88.507
15	2.230	93.735
16	3.197	92.839

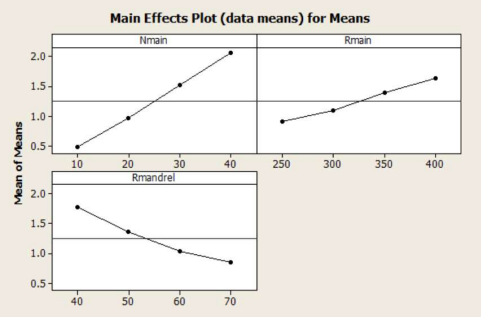

(a) V_{min}

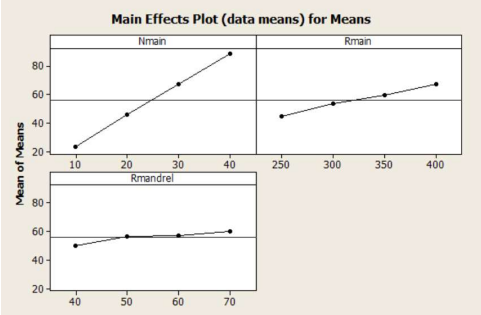

(b) V_{max}

Figure 7: Main effects plot for means

For the support ring used in powertrain systems, the process design results indicate a relatively wide range of feasible forming conditions. Therefore, the shape design of the initial ring blank (forging) before the ring rolling process is considered a relatively more important factor than the optimization of individual design variables.

2.5 Cross-sectional Shape Design of Ring Blanks for Profile Ring Rolling Process

The basic concept of the uniform volume distribution element technique (UVDET) is to divide a ring blank into several regions using linear elements and to predict the metal flow between these regions **[11]-[12]**. Throughout the ring rolling process, the cross-sectional area of the ring gradually decreases at each forming stage, and the ring diameter increases due to the incompressibility of the material. The ring blank moves across the boundary of a linear element to the adjacent-upper and lower elements while satisfying

$$\eta_h = \frac{V_{i,h} - V_{i+1,h}}{V_{i,h}} = 0 \tag{10}$$

$$V_{i,h} = \pi\left(R_{i,h}^2 - r_{i,h}^2\right), V_{i+1,h} = \pi\left(R_{i+1,h}^2 - r_{i+1,h}^2\right) \tag{11}$$

the volume constant condition. The total volume of the ring blank is calculated by summing the volumes per unit height of all linear elements. where, η_h represents the volume reduction per unit height, i.e.,

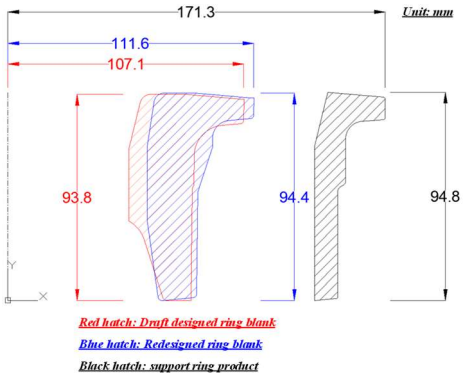

Figure 8: Cross-sectional dimensions of initial ring blanks and support ring product. (unit: mm)

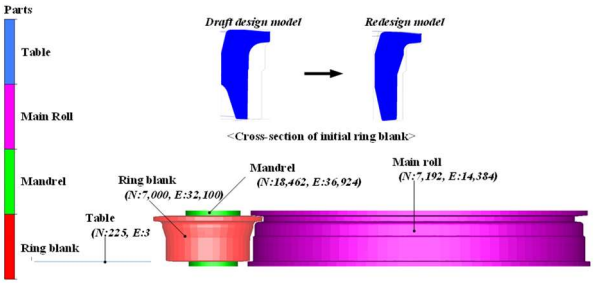

Figure 9: 3D FE-analysis model for redesigned process

the volume distribution. V and h represent the volume and height of the ring blank, respectively. The subscript i indicates the number of passes in the ring rolling process. **Figure 8** below shows the cross-sectional shape of the initial ring blank redesigned using UVDET.

3. Verification of Proposed Design Method

3.1 FE-analysis model

To validate the design of the profile ring rolling process, applying a redesigned initial ring blank shape and main roll operating conditions for stable support ring manufacturing, FE-analysis was performed in the Forge Nxt 3.2 software environment. The 3D FE-analysis model was constructed similarly to "2.1.1 FE-analysis Model."

Figure 9 shows the FE-analysis model for the redesigned process. The number of nodes and elements in the initial ring blank is 7,000 and 32,100, respectively. Principal process variables are listed in **Table 1**, and the feed rate of the main roll proposed under the feasible forming conditions is shown in **Figure 10**.

3.2 Result of FE-analysis

The results of the FE-analysis performed with the proposed process conditions using the feasible forming condition and UVDET are summarized in **Figures 11** and **12**, which show the shape change, effective strain distribution, and temperature distribution of the

support ring product, respectively.

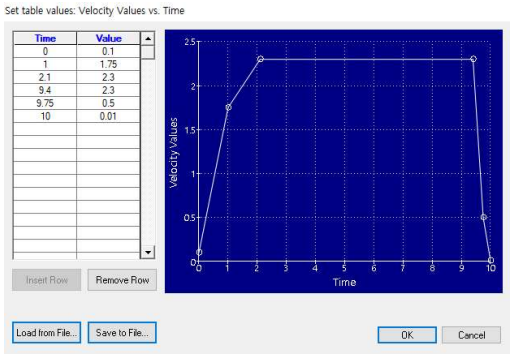

Figure 10: Set table values: Feed rate of main roll vs time

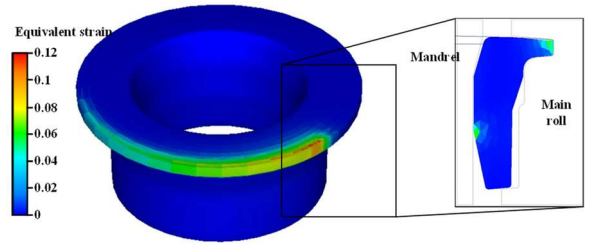

(a) 2.5 sec

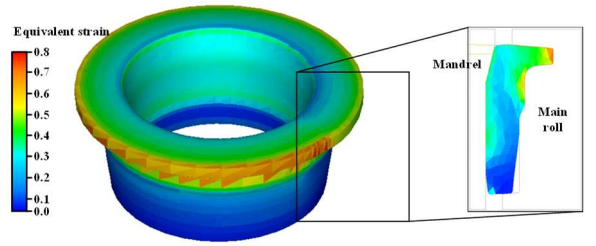

(b) 5 sec

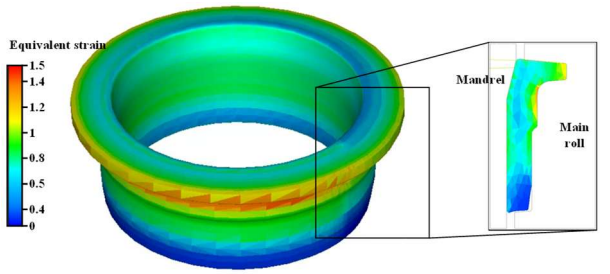

(c) 7.5 sec

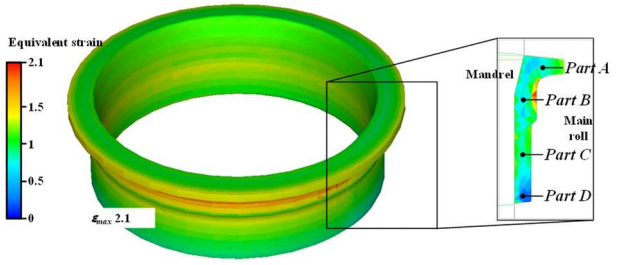

(d) 10 sec

Figure 11: Plastic zone distribution of deformed support ring during the redesigned process

The effective strain distribution for each step was confirmed by setting it to auto range, and the maximum strain of the support ring was observed to be 2.1 in the last step (15 sec). As can be seen in the plastic zone distribution in **Figure 11**, the plastic zone was first generated on the outer surface of the upper part (*Part A*) of the support ring and the inner surface of the middle part (*Part C*) when the roll feed was small. As the feed increased, the upper part (*Part A*) and the middle parts (*Parts B, C*) of the support ring were filled, and then the contact (deformation) zone was gradually created toward the lower part (*Part D*). The stable forming was achieved without defects such as lifting, under-filling, and over-filling at the lower part of the support ring that occurred under the existing field try-out conditions. However, a slight under-filling defect appeared on the outer surface of the support ring protrusion.

The temperature distribution in **Figure 12** shows that the ring temperature after the hot ring rolling process ranges from 876.2˚C to 913.4˚C. A relatively high temperature distribution is observed in the middle sections of the support ring (*Parts B* and *C*), where the greatest plastic deformation is expected, and the temperature decreases toward the lower part of the ring (*Part D*). However, due to the short forming time, the initial ring blank temperature of 900˚C did not change significantly.

4. Conclusion

In this study, the process design method for the pure-radial vertical profile ring rolling process is proposed. The effectiveness of the proposed method was verified through 3D FE-analysis of the support ring manufacturing process. Key conclusions are as follows.

(1) To reduce ring spreads and maintain process stability, we developed the feasible forming condition for a single-stage vertical ring rolling process. Based on mathematical modeling that comprehensively considers plastic penetration and force balance, feasible forming conditions were derived, which are expressed in **Equations (6)**, **(8)**, and **(9)**.

(2) To reduce ring spreads and maintain process stability, we developed the feasible forming condition for a single-stage vertical ring rolling process. Based on mathematical modeling that comprehensively considers plastic penetration and force balance, feasible forming conditions were derived, which are expressed in **Equations (6)**, **(8)**, and **(9)**.

(3) The cross-sectional shape design of the initial ring blank for the profile ring rolling process was performed using

the UVDET, and its effectiveness was confirmed by observing the expansion of the plastic zone during the whole process. However, further research is needed to select the ring blank shape in conjunction with the hot forging process before the ring rolling process.

(4) The proposed design method ensured a successful ring shape and excellent dimensional accuracy. These research results can serve as basic guidelines for process design during actual on-site try-out operations.

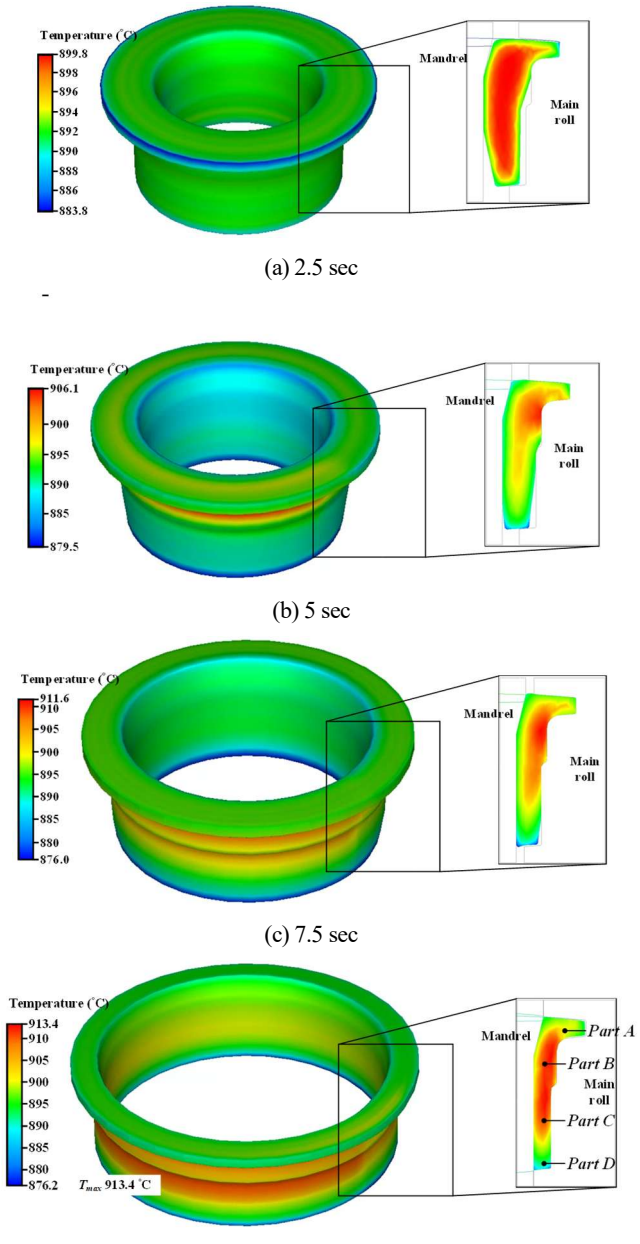

Figure 12: Temperature distribution of deformed support ring during the redesigned process

Acknowledgement

This study has been conducted with the support of the Korea Institute of Industrial Technology as "Development of Platform Core Technology of Smart Manufacturing System of Hot Composite Forming Process for manufacturing support ring based on Artificial Neural Network (KITECH-JH230007).

Author Contributions

Conceptualization, I. K. Lee and K. H. Lee; Methodology, S. K. Lee and K. H. Lee; Software, K. H. Lee; Validation, I. K. Lee and S. K. Lee; Data Curation, I. K. Lee and S. Y. Lee; Writing—Original Draft Preparation, I. K. Lee; Writing—Review & Editing, K. H. Lee; Visualization, K. H. Lee; Supervision, K. H. Lee.

References

[1] E. Eruc and R. Shivpuri, “A summary of ring rolling technology-I. Recent trends in machines, processes and production lines,” International Journal of Machine Tools and Manufacture, vol. 32, no. 3, pp. 379-398, 1992.

[2] L. G. Guo and H. Yang, “Key technologies for 3D-FE modeling of radial-axial ring rolling process,” Materials Science Forum, vols. 575-578, pp. 367-372, 2008.

[3] L. Hua, L, Pan, and J. Lan, “Researches on the ring stiffness condition in radial-axial ring rolling,” Journal of Materials Processing Technology, vol. 209, no. 5, pp. 2570-2575, 2009.

[4] G. Zhou, L. Hua, J. Lan, and D. S. Qian, “FE analysis of coupled thermos-mechanical behaviors in radial-axial rolling of alloy steel large ring,” Computational Materials Science, vol. 50, no. 1, pp. 65-76, 2010.

[5] K. H. Lee and B. M. Kim, “Advanced feasible forming conditions for reducing ring spreads in radial-axial ring rolling,” International Journal of Mechanical Sciences, vol. 76, pp. 21-32, 2013.

[6] D. H. Lee, B. M. Kim, and K. H. Lee, “Design of pure-radial ring rolling process by using advanced feasible forming condition,” Journal of the Korean Society of Marine Engineering, vol. 42, no. 4, pp. 287-292, 2018 (in Korean).

[7] L. Li, H. Yang, L. Guo, and Z. Sun, “Research on interactive influences of parameters on T-shaped cold ring rolling by 3d-FE numerical simulation,” Journal of Mechanical Science and Technology, vol. 21, pp. 1541-1547, 2007.

[8] K. H. Kim, H. G. Suk, and M. Y. Huh, “Development of the profile ring rolling process for large slewing rings of alloy steels,” Journal of Materials Processing Technology, vols. 187-188, no. 12, pp. 730-733, 2007.

[9] D. S. Qian, L. Hua, and L. B. Pan, “Research on gripping conditions in profile ring rolling of raceway groove,” Journal of Materials Processing Technology, vol. 209, no. 6, pp. 2794-2802, 2009.

[10] M. C. Park, C. J. Lee, J. M. Lee, I. K. Lee, M. S. Joun, B. M. Kim, and K. H. Lee, “Development of L-sectioned ring for construction machines by profile ring rolling process,” International Journal of Precision Engineering and Manufacturing, vol. 17, no. 2, pp. 233-240, 2016.

[11] K. H. Lee, D. C. Ko, D. H. Kim, S. B. Lee, N. M. Sung, and B. M. Kim, “Design method for intermediate roll in multi-stage profile ring rolling process: the case for excavator idler rim,” International Journal of Precision Engineering and Manufacturing, vol. 15, no. 3, pp. 503-512, 2014.

[12] B. M. Kim and K. H. Lee, “Roll design method of single-stage profile ring rolling based on modified UVDET,” Key Engineering Materials, vols. 622-623, pp. 1008-1014, 2014.